International Journal of Mechanical and Civil Engineering
ISSN: 2689-940X
Volume 5, Issue 1, 2022 (pp. 55-72)
www.abjournals.org

THE USE OF X-RAY COMPUTED TOMOGRAPHY FOR THE ASSESSMENT OF THE INTERNAL STRUCTURE OF CARBONATED SOIL

Amos Yala Iorliam[1*], Ajibola Rasaq Lawal [2] and Rilwanu Ibrahim[3]

[1]Department of Civil Engineering, Joseph Sarwuan Tarka University Makurdi, P.M.B. 2373, Makurdi, Nigeria (Formerly Department of Civil Engineering, Federal University of Agriculture Makurdi, P.M.B. 2373, Makurdi, Nigeria.

[2]Faculty of Civil Engineering, Wroclaw University of science and technology, Wroclaw, Poland.

[3]Works Department, Federal University of Lafia, PMB 146, Lafia Nasarawa State, Nigeria.

*Corresponding author's E-mail: amosyalas2007@yahoo.com

Cite this article:

Iorliam A.Y., Lawal A.R., Ibrahim R. (2022), The use of X-Ray Computed Tomography for the Assessment of the Internal Structure of Carbonated Soil. International Journal of Mechanical and Civil Engineering 5(1), 55-72. DOI: 10.52589/IJMCE-A1HGJX8L.

Manuscript History

Received: 1 Oct 2022

Accepted: 29 Oct 2022

Published: 19 Nov 2022

ABSTRACT: *This study looks at the use of X-ray computed tomography (XRCT) technique to determine the internal structure of carbonated lime treated kaolin. The results show that the formation of calcium carbonate ($CaCO_3$) along the depth of carbonated kaolin can be determined using XRCT. The carbonate formed shows to be evenly distributed deep down the lime treated kaolin. The air voids of carbonated lime treated kaolin decreased compared to the corresponding non-carbonated lime treated kaolin. $CaCO_3$ content obtained from XRCT compared favourably with that from TGA and calcimeter technique. XRCT has the potential for the determination of internal structure of carbonated lime treated soil.*

KEYWORDS: X-ray computed tomography, lime treated kaolin, calcium carbonate content, air voids content.

Article DOI: 10.52589/IJMCE-A1HGJX8L
DOI URL: https://doi.org/10.52589/IJMCE-A1HGJX8L

International Journal of Mechanical and Civil Engineering
ISSN: 2689-940X
Volume 5, Issue 1, 2022 (pp. 55-72)

www.abjournals.org

INTRODUCTION

The determination of calcium carbonate in soils and stabilised soils is well known. This enables the assessment of carbon capture potential in soils. Carbon capture and storage in soils is one means of reducing excess atmospheric carbon dioxide (CO_2) concentrations for climate change mitigation usually caused by human activities (Lal, 2004; Dorr, 2016).

Several methods have been used in assessing the presence, content and morphology of carbonate in soils. Some of the methods as presented in Table 1 include X-ray diffraction (XRD), thermogravimetric analysis (TGA), Phenolphthalein alcoholic solution, scanning electron microscopy (SEM) and energy-dispersive X-ray spectroscopy (EDX) (Al-Mukhtar *et al*., 2012; Nakarai & Yoshida, 2015; Washbourne *et al*., 2015; Iorliam *et al.* 2021). Generally, properties, such as calcium carbonate ($CaCO_3$) content, have been determined using TGA and calcimeter. Also, chemical composition of $CaCO_3$ has been obtained using SEM and EDX, mineralogical composition of $CaCO_3$ has been achieved using TGA and XRD, while surface appearance has been ascertained through SEM. However, reports on the use of XRCT for the determination of internal structure of carbonated soil is scarce. This prompted the current study on the use of XRCT for the determination of internal structure of carbonated soil.

The aim of this study is to determine whether the internal structure of carbonated soil can be determined using XRCT. The specific objectives are to examine the changes in $CaCO_3$ and air voids contents in carbonated soil and compare with these in the equivalent non-carbonated soil.

Table 1: Previous Studies on Determination of Calcium Carbonate in Soils

Author	Title	Assessment method	Property found
Eades *et al*. (1962)	Formation of new minerals with lime stabilization as proven by field experiments in Virginia	XRD was used to investigate the presences of Calcium carbonate ($CaCO_3$) in lime treated subgrade soils at three project sites in Virginia.	$CaCO_3$ mineral content was determined using XRD. Approximately 2.5% $CaCO_3$ was obtained in 5% $Ca(OH)_2$ treated subgrade soil.
De Silva *et al*. (2006)	Carbonate binders: reaction kinetics, strength and microstructure	SEM and EDX were used to examine compacted lime with different water/solid (W/S) ratios and various compaction densities.	Morphologies and chemical composition of $CaCO_3$ content were determined from the lime compacts based on W/S ratios and compaction densities using SEM and EDX respectively.

Article DOI: 10.52589/IJMCE-A1HGJX8L
DOI URL: https://doi.org/10.52589/IJMCE-A1HGJX8L

Cizer *et al*. (2010)	Competition between hydration and carbonation in hydraulic lime and lime-pozzolana mortars	XRD and TGA were used to assess mortars made with hydraulic lime and lime pozzolana.	Calcite mineral phase was determined using XRD. $CaCO_3$ was determined due to carbonation reaction using TGA.
Al-Mukhtar *et al*. (2012)	Microstructure and geotechnical properties of lime-treated expansive clayey soil	XRD and TGA were used to examine lime treated natural clayey soil.	$CaCO_3$ mineral was determined from carbonated lime ($Ca(OH)_2$) treated clay using XRD and TGA patterns.
Nakarai and Yoshida (2015)	Effect of carbonation on strength development of cement treated Toyoura silica sand	TGA and phenolphthalein alcoholic solution were used to examine carbonated cement treated Toyoura silica sand. The varying carbonation curing were natural (≈0.03%) and 5% CO_2	Using TGA, the rate of carbonation reaction was found to be influenced by CO_2 concentration. The carbonation of 8% cement treated Toyoura silica sand under approximately 5% CO_2 curing condition achieved approximately 40% $CaCO_3$ content within 91 days. However, the carbonation of equivalent cement treated soil under approximately 0.03% CO_2 ($natural\ atmospheric$) curing achieved similar $CaCO_3$ content (40%) in 365 days. The carbonation depth was determined using phenolphthalein alcoholic solution.
Washbourne *et al*. (2015)	Rapid removal of atmospheric CO_2 by urban soils	TGA, calcimeter and XRD were used to determine $CaCO_3$ contents in soils made up of demolition rubbles containing fragments of building materials.	The presence of $CaCO_3$ mineral phase was determined using XRD. Also, $CaCO_3$ presence was confirmed using SEM. The $CaCO_3$ content was determined using calcimeter and TGA.

Article DOI: 10.52589/IJMCE-A1HGJX8L
DOI URL: https://doi.org/10.52589/IJMCE-A1HGJX8L

Iorliam *et al.* (2021)	Carbon capture potential in lime modified kaolin clay	TGA, calcimeter and SEM/EDX were used to determine calcium carbonate and carbonation processes in carbonated lime treated kaolin clay.	$CaCO_3$ content was determined, e.g., the carbonation of 8% Ca($OH)_2$ treated kaolin produced 10±0.15% $CaCO_3$ content based on TGA and calcimeter analysis. Calcium carbonate formation increased with Ca($OH)_2$ contents in treated soils. The chemical composition of $CaCO_3$ was determined using SEM.

XRD = X-ray diffraction, EDX = Energy-dispersive X-ray spectroscopy, TGA = Thermogravimetric analysis

MATERIALS AND METHODS

Materials

The soil used in the current study was Imerys Polwhite Grade E kaolin clay. This clay was supplied by IMERYS Minerals Ltd, United Kingdom (UK). The mechanical and chemical compositions of the clay are presented in Table 2. The lime used was $Ca(OH)_2$ supplied by Lafarge Tarmac Cement & Lime, Buxton, UK. The chemical composition of the lime as provided by the manufacturer is also presented in Table 2. Sodium carbonate used in this study was supplied by VWR International, UK. The chemical composition is again shown in Table 2.

Methods

A series of laboratory experiments were conducted to assess the internal structure of carbonated lime treated kaolin using XRCT. Kaolin was treated with lime to achieve soil modification in accordance with BS 1924-2 (BSI, 2018). The treated kaolin was subjected to carbonation treatment to achieve carbonated lime treated kaolin. Thereafter, the carbonated treated kaolin was examined under XRCT to determine their internal structure.

Table 2: Physical and chemical properties of kaolin (Polwhite E), lime and sodium carbonate as used in the current study

Property	Kaolin	Lime	Sodium Carbonate
Chemical composition[a]			
SiO_2(mass %)	50	0.7	0.00005
Al_2O_3 (mass %)	35	0.1	-
Fe_2O_3(%)	-	0.06	-
$Ca(OH)_2$ (%)	-	96.9	
$Mg(OH)_2$ (%)	-	0.5	

Article DOI: 10.52589/IJMCE-A1HGJX8L
DOI URL: https://doi.org/10.52589/IJMCE-A1HGJX8L

$CaSO_4$ (%)	-	0.03	
Mn (%)	-	175 ppm	
F (%)	-	65 ppm	
Pb (%)	-	1.3 ppm	
As (%)	-	0.3 ppm	
Free moisture (%)	-	0.25	
Assay (dried basis)	-	-	99.5% Na_2CO_3min
SO_4	-	-	0.003% max
Chloride (Cl)	-	-	0.001% max
Phosphate (PO_4)	-	-	0.001% max
Iron (Fe)	-	-	5 ppm max
Calcium (Ca)	-	-	0.03% max
Magnesium (Mg)	-	-	0.005%
Potassium (K)	-	-	0.005 (%)
Insoluble matter	-	-	0.01% max
Loss on heating at 285^oC	-	-	1.0% max
Physical properties:			
0.06–0.002 mm (%)	65		
Less than 0.002 mm (<2 µm) (%)	35		
Surface area (BET; m^2/g)	8		
pH	5.5		
Cation exchange capacity (cmol/kg)	4.0		
Specific gravity	2.6		
Liquid limit (%)	59		
Plastic limit	31		
Plasticity index (%)	28		
Optimum moisture content (%)	26.5		
Maximum dry density (Mg/m^3)	1.44		
Initial Consumption of lime (% CaO)	3		
Unconfined compressive strength (kPa)[b]	200		

[a] Chemical analysis based on the supplier datasheet, [b] At optimum moisture content and maximum dry density.

Lime Treatment for Soil Modification

To achieve soil modification, kaolin was treated with lime based on the result of the modified initial consumption of lime (ICL) test, according to the definition by Rogers *et al*. (1997). The ICL value obtained was 4% $Ca(OH)_2$ by dry mass, which is equivalent of 3% calcium oxide (CaO) content. Details of this are contained in Iorliam (2019). Therefore, kaolin clay was treated for modification by addition of $Ca(OH)_2$ from 4% (ICL value equivalent), 6% (ICL+1.5% CaO) and 8% (ICL+3% CaO) $Ca(OH)_2$. Lime, kaolin and water were mixed and compacted based on set range of water contents and densities (Table 3) obtained in accordance with the normal Proctor (light) compaction method (BS 1377, 2016). This was to achieve compacted lime treated kaolin for the set water contents and densities as shown in Table 3.

Article DOI: 10.52589/IJMCE-A1HGJX8L
DOI URL: https://doi.org/10.52589/IJMCE-A1HGJX8L

International Journal of Mechanical and Civil Engineering
ISSN: 2689-940X
Volume 5, Issue 1, 2022 (pp. 55-72)

www.abjournals.org

Compacted lime treated kaolin will henceforth be referred to as treated kaolin. The mixture were then tamped into a split mould of dimensions 38 mm diameter and 76 mm length in three layers to achieve the desired densities and air voids shown in Table 3. Specimens were immediately placed in 38 mm PVC plastic specimen tubes and the ends sealed with wax for curing. Specimens were cured in a temperature-controlled room (20^{o}C and 55% relative humidity) for 7 days at the Geotechnical Engineering Laboratory, Department of Civil Engineering and Geosciences, University of Newcastle upon Tyne, UK. Curing for 7 days allows for short term reactions which are often considered as modification reactions (Jung & Bobet, 2008). These specimens were used for carbonation treatment.

Table 3: Compaction target data for soil modification

Calcium hydroxide content (%)	Air void content (%)	Water content (%)	Dry density (Mg/m^3)	Bulk density (Mg/m^3)	Bulk mass (g)
0	3 [a]	26[b]	1.442	1.817	157
4	3 [a]	29[b]	1.435	1.8512	160
	10	26	1.405	1.7703	152
	15	23	1.38	1.6974	147
	20	21	1.354	1.6383	141
	25	18	1.335	1.5753	136
6	3 [a]	30[b]	1.425	1.8525	159
	10	26	1.395	1.7577	152
	15	24	1.367	1.6951	146
	20	21	1.342	1.6238	140
	25	18	1.32	1.5616	135
8	3 [a]	30 [b]	1.418	1.8434	159
	10	26	1.389	1.7501	151
	15	24	1.360	1.6864	145
	20	22	1.328	1.6202	139
	25	19	1.306	1.5541	134

[a]Air void at maximum dry density (MDD), [b]Moisture content at optimum moisture content (OMC)

Carbonation Treatment

To form carbonated treated kaolin specimens, a carbonation treatment experiment was conducted on post modified treated kaolin specimens based on the permeability in a triaxial cell test in accordance with BS 1377 (BSI, 2016) at the Geotechnical Engineering Laboratory, Department of Civil Engineering and Geosciences, UK. The triaxial cell used in this study was fitted with a measurement and control system (Geotechnical Digital Systems: GDS) having automatic pressure and volume control units (Figure 1). More details of the carbonation process are contained in Iorliam (2019).

Article DOI: 10.52589/IJMCE-A1HGJX8L
DOI URL: https://doi.org/10.52589/IJMCE-A1HGJX8L

International Journal of Mechanical and Civil Engineering
ISSN: 2689-940X
Volume 5, Issue 1, 2022 (pp. 55-72)
www.abjournals.org

To perform the carbonation treatment, some adjustments to the triaxial cell were carried out. This was to allow for high carbon (HC) solution (1 molar $NaCO_3$) to permeate through the treated kaolin specimen to achieve accelerated carbonation.

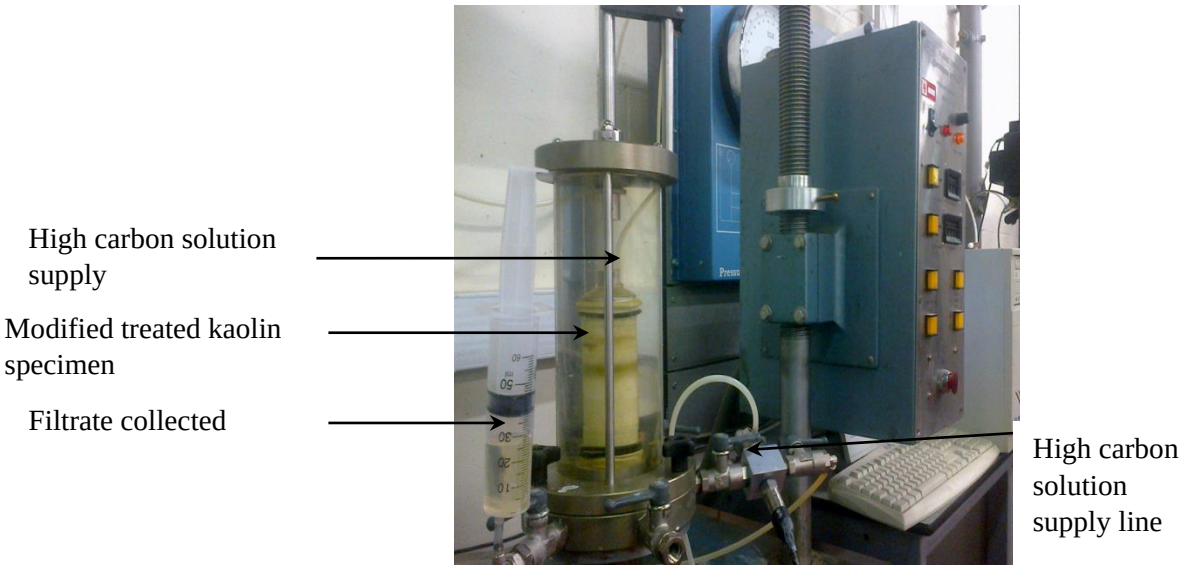

Figure 1: Carbonation treatment of calcium hydroxide treated kaolin clay using triaxial cell set-up (modified from BS 1377-6: BSI 2016).

A storage tank was added to the triaxial cell arrangement, to accommodate the HC solution. The tank was connected to the volume change gauge, and then to pore-pressure line onto the top cap of the cell for supply of HC solution (under constant pressure) onto the top of the specimen. An air-tight syringe was connected to the drainage line to collect filtrate from the specimen. The modified treated kaolin specimen was placed on the pedestal in the triaxial cell according to BS 1377 (BSI, 2016). Specimens were saturated using HC solution at Skempton's pore pressure parameter B, of at least 0.95. Fluid pressure was applied to the specimen concurrently with increased cell pressure to achieve saturation in accordance with BS 1377, part 6 (BSI, 2016). HC solution was permeated downward through the treated kaolin specimen at gauge pressure of 100 kPa and cell confining pressure of 150 kPa. The filtrate was collected through the syringe at intervals of 1 hour until the carbonation treatment was completed. The carbonation treatment was considered completed when the electrical conductivity (EC) of the filtrate was the same as that of the supplied HC solution. The EC of the filtrate from the specimen was determined in accordance with BS EN 7755–3.4 (BSI 1995a) using a microprocessor controlled electrical conductivity/TDS meter (HANNA HI 9835 model).

Article DOI: 10.52589/IJMCE-A1HGJX8L
DOI URL: https://doi.org/10.52589/IJMCE-A1HGJX8L

International Journal of Mechanical and Civil Engineering
ISSN: 2689-940X
Volume 5, Issue 1, 2022 (pp. 55-72)

www.abjournals.org

X-ray Computed Tomography Scanning

To assess changes in the internal structure (such as voids, carbonates contents) of carbonated treated kaolin samples, the samples were scanned using an Zeiss VersaXRM410 XRCT scanner (Durham University School of Engineering and Computing Sciences, UK). Due to cost and time involved, XRCT scanning was performed on 1 non-carbonated treated and 9 carbonated treated kaolin samples, as presented in Table 4. The non-carbonated treated sample served as a control. Samples were selected based on those with the highest strength and those at extreme and limiting air voids for $CaCO_3$ content.

The XRCT scanner has a measurement precision to 0.9 µm/pixel. High resolution scanning was required to distinguish voids spaces, $CaCO_3$ and kaolin clay particles in the sample. $CaCO_3$ grains from lime carbonation can be from 2–4 microns (De Silva *et al*., 2006), whilst particle size of kaolin clay can be up to 30 µm. Therefore, scanning resolution of 1 pixel to 2.5 µm for the sample scan was selected. This scan was intended to distinguish the particles of $CaCO_3$, kaolin clay and voids spaces in the sample.

It is recommended that the specimen be of the order of 1,000 times larger than the desired resolution for XRCT scanning (Ketcham & Carlson, 2001). To prepare samples for high resolution scanning, a core sample of 5 mm diameter and 25 mm height was obtained from parent carbonated treated kaolin sample (38 mm diameter, 76 mm height) (Figure S1a in Supplementary Materials). Plastic tube (5 mm diameter, 25 mm height) was axially driven through the central carbonated treated kaolin sample, and the core sample was recovered in the plastic tube (Figure S1b in Supplementary Materials). The sample was then used for scanning and resulting images were obtained for analysis.

Table 4: List of carbonated and non-carbonated samples tested using X-ray computed tomography

Sample name	Sample description		
	Carbonated sample	Non-carbonated sample	Notes
4L3AV	4% $Ca(OH)_2$ content at 3% air voids content	–	Sample at lowest air voids
6L3AV	6% $Ca(OH)_2$ content at 3% air voids content	–	Sample at lowest air voids
8L3AV	8% $Ca(OH)_2$ content at 3% air voids content	–	Sample at lowest air voids
4L10AV	4% $Ca(OH)_2$ content at 10% air voids content	–	Sample at air voids with highest strength in 4% $Ca(OH)_2$ content
6L10AV	6% $Ca(OH)_2$ content at 10% air voids content	–	Sample at air voids with highest strength in 6% $Ca(OH)_2$ content
8L10AV	8% $Ca(OH)_2$ content at 10% air voids content	8% $Ca(OH)_2$ content, at 10% air voids content	Sample at air voids with highest strength in 8% $Ca(OH)_2$ content (only in carbonated sample)

Article DOI: 10.52589/IJMCE-A1HGJX8L
DOI URL: https://doi.org/10.52589/IJMCE-A1HGJX8L

4L25AV	4% $Ca(OH)_2$ content at 25% air voids content	–	Sample at highest air voids
6L25AV	6% $Ca(OH)_2$ content at 25% air voids content	–	Sample at highest air voids
8L25AV	8% $Ca(OH)_2$ content at 25% air voids content	–	Sample at highest air voids

X-ray Computed Tomography Analytical Procedure

To analyse the XRCT data of carbonated treated kaolin, images of t scanned samples were reconstructed using ImageJ (v.1.43u) software (Rasband, 2002), such as the reconstruction performed by Beckett *et al*. (2013). An overview of the images for analysis is presented in Figures S2 and S3 in Supplementary Materials, while the flowchart of the XRCT data processing using ImageJ is included in Figure S4 in Supplementary Materials.

Firstly, the first and last 100 image slices were deleted from the data sequence. Removal of first and last 100 slices from the sequence was required to prevent shadowing, as also carried out by Beckett *et al*. (2013), and Smith and Augarde (2014). The removal of these extreme slices also reduces the chance of damaged materials likely to be found at the ends of the sample from affecting the analysis. In this study, 900 slices were available after the removal of extreme slices. This was required so that measurement of result can be presented in calibrated real value (μm in this case).

The images were converted from 32 bit to 8 bit. Converting the image to 8 bit greyscale meant that there are 256 intensity values which can be assigned to a pixel. This was required for two reasons: Firstly, to fit into thresholding window (ImageJ) which requires 256 grey shades. Secondly, converting from original 32 bit data to 8 bit data has an advantage of reducing the data size. For example, 15.4 MB/slice in 32 bit data was reduced to 3.9 MB/slice in 8 bit data format. This assists in speeding up ImageJ software analysis and improves data handling.

Cropping of image slice was performed on a typical carbonated treated kaolin image. This was required to avoid shadowing at the sample edges. It further reduced data size, for example cropping a 5 mm diameter slice to square (3.3 mm × 3.3 mm) image, and reduced the size from 1004 kb to 413 kb (Figures S2c and Figure S2b in Supplementary Materials).

Additionally, filtering the image was carried out in order to reduce noise and enhance sample features. The “adaptive median” filter was applied to the sample image to remove the outlying intensity regions as also performed by Beckett *et al*. (2013). This filter method removes the extreme outliers from the image whilst preserving the original details. It replaces a pixel being considered with a pre-selected median pixel value. A pixel is square shaped; to keep the pixel entries intuitively similar to the neighbouring pixels and at the same time keep the edges not eroded, adaptive median filter was required. This median filter radius defines the size of a square pixel and preserve the small details of original image (Khryashchev *et al*., 2005). In this study 2.0 pixels radius was applied such as also applied in the study of Beckett *et al*. (2013). A typical filtered image is contained in Figure S2d in Supplementary Materials.

Furthermore, setting a threshold value (Figure S2f in Supplementary Materials) was applied to the images. This was essential to separate pixels which fall within a desired range of intensity

Article DOI: 10.52589/IJMCE-A1HGJX8L
DOI URL: https://doi.org/10.52589/IJMCE-A1HGJX8L

values from those which do not. The converted image to 8-bits grey scale turns pixel with the lowest value of zero (0) to black and pixel with highest intensity of 255 to white, while every pixel intensity between 0 and 255 is a shade of grey.

Ten different randomly located small regions for each sample were taken and an operator selected threshold value was obtained as performed by Smith & Augarde (2014). The threshold value was then applied to the entire slices in the sequence, resulting in two phase separation.

For the measurement of air voids content, threshold values were applied for all the samples which separated voids from solid material areas. Voids areas showed black, whilst areas of solid materials (kaolin plus carbonate) showed white (Figure S2g in Supplementary Materials).

For measurement of the desired feature in an image, it was required to select the perimeter around the feature for measurement. The selection was to isolate the features for measurement and the desired information (such as area, minimum and maximum grey value) recorded. A typical selection of properties (voids spaces) is shown in Figure S2h in Supplementary Materials.

For the determination of carbonate content, a threshold intensity value was applied to distinguish carbonate and non-carbonate phases. A preliminary threshold intensity value was selected from the histogram of the corresponding carbonated sample image.

Typical XRCT scan images of non-carbonated and carbonated samples made of 8%$Ca(OH)_2$ and 10% air voids (8L10AV) are contained in Figures S3a and S3b respectively in Supplementary Materials. For the analysis of carbonated 8L10AV treated kaolin, the threshold value that identified the calcite was >125. When thresholding was applied, the XRCT image was divided into foreground and background (Figures S3c and S3d in Supplementary Materials). The identified white particles represent the presence of calcite formed and the black regions represent the soil (Figure S3d in Supplementary Materials).

For measurement of image parameters (such as void and carbonate areas), only one per every ten images was processed due to the large number of sample images, as also performed by Beckett *et al*. (2013). For example, 90 images were analysed out of 900 images available in this study.

Voids content (% by volume) was determined using Equation 1.

$$\text{Voids contents (\% by volume)} = \frac{detected\ area\ of\ voids \times sample\ thickness}{Total\ area\ of\ sample \times sample\ thickness} \quad (1)$$

Carbonate contents (% by mass) was determined using Equation 2

$$\text{Carbonate contents (\% by mass)} = \frac{detected\ area\ of\ calcite \times sample\ thickness \times density\ of\ calcite}{Total\ area\ of\ non{-}calcite \times sample\ thickness \times\ density\ of\ clay} \quad (2)$$

One of the acceptable techniques to determine different phases in solid images is the threshold technique. The manufacturers of ImageJ stated that "if other parameters than the intensity define the structure outline or area, a simple threshold does not lead to satisfying results or even fails completely doing the job" (ImageJ, 2016). Furthermore, Smith (2015), in the study of soil based construction materials using XRCT, pointed out that "unfortunately however, the use of

Article DOI: 10.52589/IJMCE-A1HGJX8L
DOI URL: https://doi.org/10.52589/IJMCE-A1HGJX8L

a single threshold still produced some uncertainties in the final conclusion." Based on the fact that a single threshold cannot work on all the samples to determine the presence of calcite formed as pointed by ImageJ (2016) and Smith (2015), different thresholds were used for the analysis of different images.

Comparison of Calcium Carbonate Content from XRCT with Geochemical Testing

For the purposes of comparison, results of $CaCO_3$ contents from geochemical testing such as TGA and calcimeter obtained from the same specimens used for XRCT analysis by Iorliam (2019) were used. The results of $CaCO_3$ contents from XRCT in the current study were compared with those from calcimeter and TGA.

Additionally, theoretical $CaCO_3$ content was determined based on stoichiometry, as presented in Equation 3. Theoretical $CaCO_3$ content refers to the amount of carbonates that would be formed if a complete carbonation of available cations was achieved (Matsushita *et al.*, 2000)

$$Ca(OH)_2 + CO_2 \rightarrow CaCO_3 + H_2O \quad (3)$$

A T-test was conducted on the results of $CaCO_3$ from XRCT, TGA and calcimeter to determine whether the results from XRCT and the other methods were similar.

The T-test was calculated from Equation 4.

$$T = \frac{\underline{d}}{SE(\underline{d})} \quad (4)$$

where $\underline{d}$ represents the mean difference, $SE(\underline{d}) = \frac{S_d}{\sqrt{n}}$ represents the standard error of the mean difference, S_d denotes the standard deviation of the differences, n stands for the sample size, and t represents t quantile with n-1 degrees of freedom.

RESULTS AND DISCUSSION

Variation of Calcium Carbonate Content with Sample Depth using XRCT

Figure 2 presents the results of detected $CaCO_3$ with depth in treated kaolin using XRCT for 90 slices per sample. The results show that $CaCO_3$ formed is distributed relatively even through the depth of the treated kaolin specimen.

Article DOI: 10.52589/IJMCE-A1HGJX8L
DOI URL: https://doi.org/10.52589/IJMCE-A1HGJX8L

International Journal of Mechanical and Civil Engineering
ISSN: 2689-940X
Volume 5, Issue 1, 2022 (pp. 55-72)
www.abjournals.org

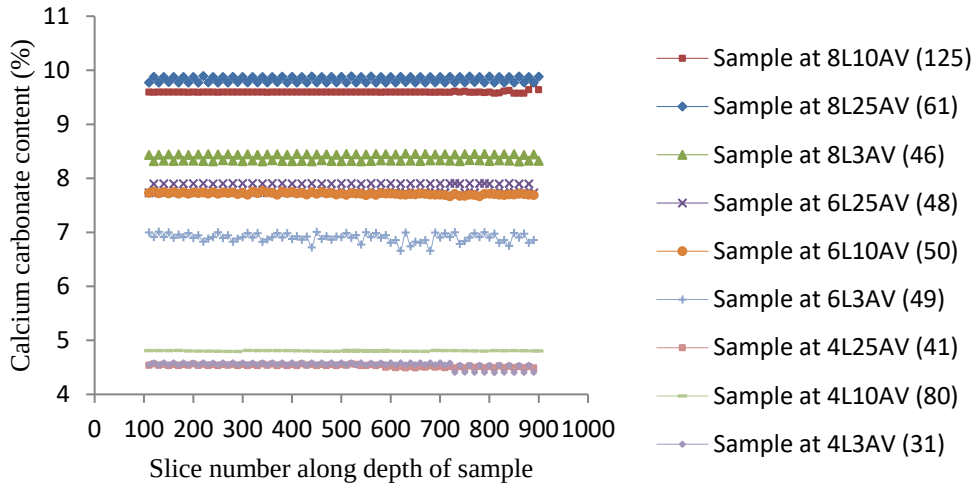

Figure 2: Calcium carbonate content variation with sample slices of carbonated treated kaolin.

Note: Threshold values are given in parentheses. L represents percentage calcium hydroxide content; AV represents percentage air void content.

This indicates that by design, carbonate formation could be distributed deep down the lime treated cohesive soil based on the volume of the soil required. To the best of the researchers' knowledge, the use of XRCT to measure the amount of carbonate in lime modified soil is being performed for the first time.

Comparison of Calcium Carbonate Content using XRCT, TGA and Calcimeter Methods

The experimental results showing $CaCO_3$ content determined from XRCT analysis are presented in Table 5. For comparison, $CaCO_3$ content, determined from calcimeter and TGA analysis from equivalent samples as contained in Iorliam (2019), is also presented in Table 5. The results of theoretical $CaCO_3$content again is shown in Table 5. The results which are on samples at 10% air voids content show that $CaCO_3$ content increased with increasing $Ca(OH)_2$ content. The $CaCO_3$ contents derived from XRCT show that 4.54±0.01% $CaCO_3$ content at 4% $Ca(OH)_2$ increased to 9.47±0.01% $CaCO_3$ content at 8% $Ca(OH)_2$.

To compare the similarity of $CaCO_3$ content obtained from XRCT with TGA and calcimeter methods, a t-test was performed on the $CaCO_3$ content results, again shown in Table 5. Statistical significance of the difference in $CaCO_3$ contents obtained from each pair of techniques were determined by a paired t-tests. P≤0.05 was considered to be significant. The results of t-test (Table 5) show that there was no significance difference between the results from calcimeter and XRCT at p = 0.56, TGA and XRCT at p = 0.37. Considering that, if p-value is greater than 0.05, then the results are similar (in this case results from the techniques), else they are not.

Article DOI: 10.52589/IJMCE-A1HGJX8L
DOI URL: https://doi.org/10.52589/IJMCE-A1HGJX8L

There is a reasonable agreement between XRCT technique and TGA as well as calcimeter method for determination of $CaCO_3$ content. The quantity of $CaCO_3$ derived from XRCT, TGA and calcimeter methods were comparable with that from theoretical estimation. This suggests that XRCT technique could determine $CaCO_3$ formation in soils.

Overall, the amount of $CaCO_3$ increased proportionally with $Ca(OH)_2$ content in the treated kaolin. It may be seen that doubling the $Ca(OH)_2$ additions doubles the $CaCO_3$ formed and may be predicted from Equation 3, where $Ca(OH)_2$ addition is proportional to the resulting $CaCO_3$.

The derived $CaCO_3$ content (9.47±0.01%) at 8% $Ca(OH)_2$ and 10% AV treated kaolin from XRCT method represent 87.6% compared to the theoretical derived $CaCO_3$ content (10.81%) from equivalent 8% $Ca(OH)_2$ content (Table 5). It is important to note that the amount of $CaCO_3$ formed in real world situations over time may not be as much as that obtained in the laboratory over the same time. Earlier field study by Eades *et al.* (1962) determined $CaCO_3$ content in 5% $Ca(OH)_2$ treated subgrade in road construction at Virginia after 2 years. The authors noted that 2.5% $CaCO_3$ content was achieved due to carbonation of 5% $Ca(OH)_2$ in the treated subgrade soil. This represents 50% $CaCO_3$ formation of $Ca(OH)_2$ content in 2 years. Based on the field degree of carbonation in Eades *et al.* (1962), it could be estimated that, in 2 years duration, approximately 4% of $CaCO_3$ would be produced in 8% $Ca(OH)_2$ treated clay such as kaolin in the field, due to carbonation.

Table 5: Comparison of calcium carbonate content from TGA, calcimeter and XRCT analysis for samples at 10% air voids content.

$Ca(OH)_2$ content (%)	Theoretical $CaCO_3$ (%)	[a] $CaCO_3$ content from TGA (%)	[b] $CaCO_3$ content from calcimeter (%)	[c] $CaCO_3$ content from XRCT (%)	Comparison of $CaCO_3$ results	
					TGA versus XRCT	Calcimeter versus XRCT
4	5.40	4.54±0.21	4.70±0.24	4.54±0.01	-	-
6	8.11	6.97±0.13	7.46±0.16	7.72±0.06	-	-
8	10.81	9.40±0.23	10.08±0.15	9.47±0.01	-	-
P-value					0.37	0.56

[a]Analytical error from TGA based on 1 standard deviation ranged from ±0.13 to ± 0.23 % wt $CaCO_3$. [b]Analytical error from calcimeter based on 1 standard deviation (average of 3 samples per combination) ranged from ±0.15 to ± 0.24 % wt $CaCO_3$. [c]Analytical error from XRCT based on 1 standard deviation ranged from ±0.01 to ± 0.06 % wt $CaCO_3$.

Note: TGA represents thermogravimetric analysis, XRCT represents X-ray computed tomography, $Ca(OH)_2$ represents calcium hydroxide, and $CaCO_3$ represents calcium carbonate. - represents not applicable.

Article DOI: 10.52589/IJMCE-A1HGJX8L
DOI URL: https://doi.org/10.52589/IJMCE-A1HGJX8L

International Journal of Mechanical and Civil Engineering
ISSN: 2689-940X
Volume 5, Issue 1, 2022 (pp. 55-72)
www.abjournals.org

Internal Structural Changes of Carbonated Treated Kaolin

To understand the distribution of carbonate in the treated kaolin, XRCT was used to examine images of carbonated and non-carbonated treated kaolin. Typical images showing the detected $CaCO_3$ using XRCT are presented in Figure 3. Sample at carbonated 8L10AV was selected and compared with corresponding non-carbonated 8L10AV treated kaolin. This was to assess the changes in the internal structure between the carbonated and non-carbonated samples. Sample at carbonated 8L10AV was selected to represent that with high carbonate content, while that at non-carbonated 8L10AV treated kaolin was selected to represent experimental control. The images of non-carbonated and carbonated 8L10AV treated kaolin are presented in Figures 3a and 3b respectively. On the non-carbonated treated kaolin sample (Figure 3a), the $Ca(OH)_2$ and kaolin particles are shown as light grey and dark grey respectively. Noticeable differences between carbonated sample and non-carbonate sample can be observed. There are white patches found on the carbonated sample in Figure 3b, which is lacking in the non-carbonated sample (Figure 3a). The white patches appear to be amorphous, and are suggested to be $CaCO_3$. The presence of $CaCO_3$ was unambiguously confirmed using TGA (Table 5) on the same specimen used for XRCT and is reported in details by Iorliam (2019).

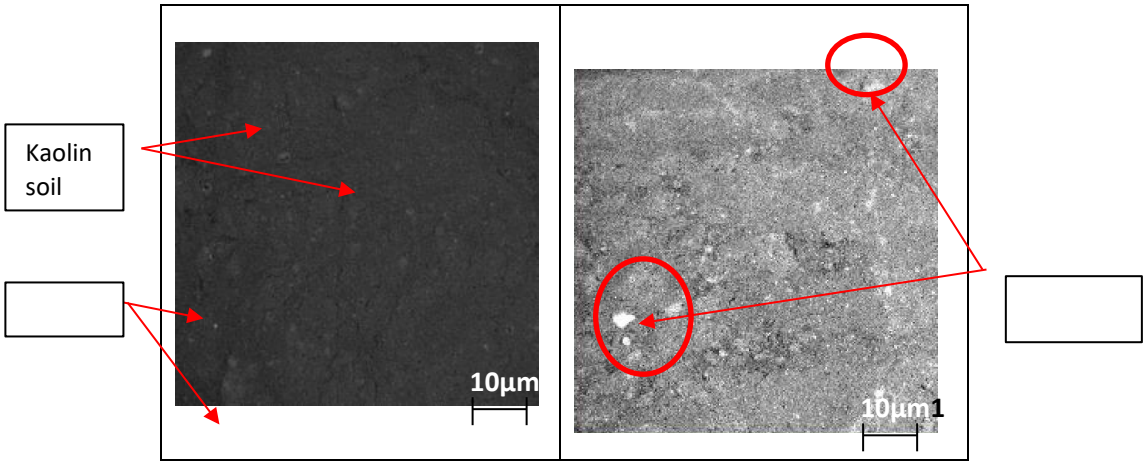

Figure 3: XRCT Images of 8L10AV (8% calcium hydroxide, 10% air voids) treated kaolin (a) non-carbonated sample (b) carbonated treated sample.

Note: White patches represents calcium carbonate particles. The red circles mark typical areas where calcium carbonate is suggested to be formed.

Reduction in Air Voids for Carbonated Samples

The results showing the detected voids content in carbonated treated kaolin using XRCT in the current study is presented in Table 6. It is shown that there is reduction in void contents for carbonated samples compared to the corresponding target air voids content at preparation for non-carbonated samples. For example, 10% air voids content for non-carbonated 8L10AV

Article DOI: 10.52589/IJMCE-A1HGJX8L
DOI URL: https://doi.org/10.52589/IJMCE-A1HGJX8L

samples is reduced to 8.32±0.07% air voids for carbonated 8L10AV samples and represents a 17% reduction in air voids content. The reduction of air voids content in carbonated samples could be due to the formation of $CaCO_3$ during carbonation of $Ca(OH)_2$ which occupies pores and reduces air voids and permeability (De Silva *et al*., 2006).

The reduction in air voids content versus target air voids at preparation for carbonated treated kaolin is presented in Figure 4. For comparison, the reduction in air voids with preparation air voids for carbonated magnesia (MgO) treated soil produced by Yi *et al*. (2015) is plotted on the same graph in Figure 4.

Table 6: Voids contents and reduction in voids of samples after carbonation

Sample Name	Target air voids content at preparation prior to carbonation (%)	XRCT determined voids content for carbonated samples (%)	XRCT determined voids content for non-carbonate samples (%)	Reduction in voids content (%)
4L3AV	3	1.95±0.01	NT	35.00
6L3AV	3	1.60±0.01	NT	46.67
8L3AV	3	1.44±0.25	NT	52.00
4L10AV	10	8.81±0.12	NT	11.9
6L10AV	10	8.78±0.07	NT	12.2
8L10AV	10	8.32±0.07	9.97 ±0.15	16.8
4L25AV	25	24.39±0.26	NT	2.44
6L25AV	25	24.09±0.08	NT	3.64
8L25AV	25	23.93±0.20	NT	4.28

Note: L represents percentage $Ca(OH)_2$ content, AV= Percentage air voids content. NT: not tested. NA= not applicable. XRCT represents X-ray computed tomography.

Reduction in air voids content is determined by the change in air voids between target air voids at preparation prior to carbonation and the post carbonation air voids, expressed as a percentage of the preparation target air voids. In the current study, the reduction in air voids content decreases as the preparation air voids content increases. This trend is consistent with the results from the study on carbonation of MgO treated soil by Yi *et al.* (2015) (Figure 4). This indicates that carbonated treated kaolin would contain less air voids content than thecorresponding non-carbonated treated kaolin.

Article DOI: 10.52589/IJMCE-A1HGJX8L
DOI URL: https://doi.org/10.52589/IJMCE-A1HGJX8L

International Journal of Mechanical and Civil Engineering
ISSN: 2689-940X
Volume 5, Issue 1, 2022 (pp. 55-72)

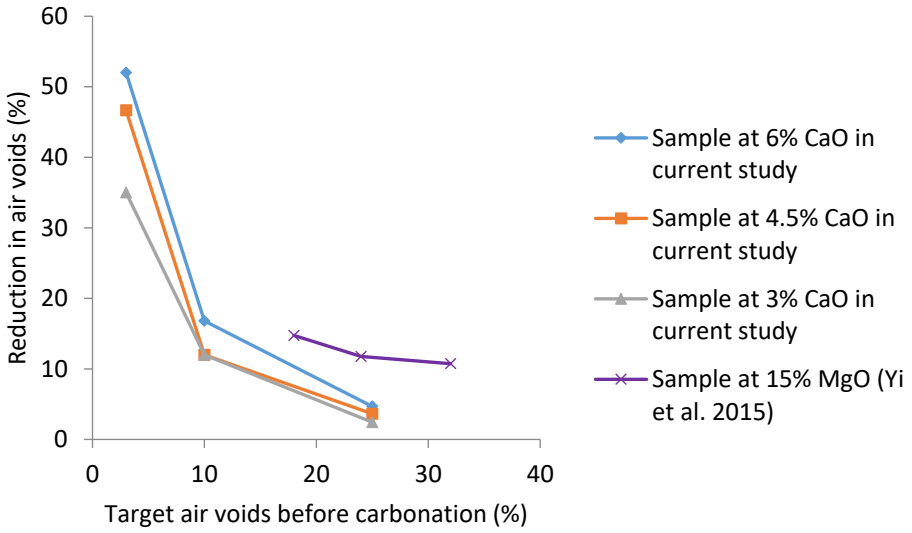

Figure 4: Reduction in air voids as a function of carbonation of calcium oxide treated kaolin clay in the current study and of magnesium oxide (MgO) treated lean clay soil produced by Yi *et al.* (2015).

CONCLUSIONS

The current study addressed the assessment of the internal structure of carbonated lime treated kaolin using XRCT technique. From the results, the following conclusions can be drawn:

- The formation of $CaCO_3$ along the depth in carbonated treated kaolin could be determined using XRCT. The carbonate formation shows to be evenly distributed deep down the lime treated kaolin soil, based on the volume of the treated soil.
- The $CaCO_3$ content determined using XRCT compared favourably with that determined from TGA and calcimeter techniques.
- There is a reduction in air voids contents for carbonated samples compared to the corresponding target air voids content at preparation for non-carbonated samples.
- The reduction of air voids content in carbonated samples could be due to the formation of $CaCO_3$ during carbonation of $Ca(OH)_2$ which occupies pores and reduces air voids and permeability (De Silva *et al.*, 2006).
- Based on the result from this study, XRCT technique is suitable for the determination of the internal structure of carbonated soil.

Article DOI: 10.52589/IJMCE-A1HGJX8L
DOI URL: https://doi.org/10.52589/IJMCE-A1HGJX8L

Supplement Materials

Supplementary materials containing additional figures are available at https://supplementary-materials.herokuapp.com/

Supplementary materials: Figure S1. Carbonated treated kaolin sample for XRCT scanning (a) Parent sample 38 mm diameter, 76 mm height (b) XRCT scanned sample 5 mm diameter, 25 mm height. Sample axially cored from parent sample in (a). Figure S2: ImageJ procedures on sample images: (a) sample axes (b) typical reconstructed slice xy-plane (c) cropped sample (d) post filtered image (e) enlarged section **(**f) threshold value of 46 (g) post thresholding (image pixel intensities below threshold value of 46 shown black in this case voids, whilst white spaces represents intensities above threshold value of 46, in this case solid area (h) selected areas (in orange) for measurement. Figure S3: Typical XRCT image of 8% calcium hydroxide, 10% air voids (8L10AV) treated kaolin: (a) non-carbonated sample (b) carbonated sample (c) threshold intensity of 125 on histogram. (d) Thresholded image showing black background (non-calcite), and white foreground (calcite**).** Figure S4. Procedure for XRCT data processing (using ImageJ software) (Adapted from Beckett et al., 2013).

Acknowledgement

The authors would like to thank Petroleum Technology Development Fund (PTDF), Nigeria for their financial sponsorship to the first author (AYI) to carry out this study as part of a PhD programme at the University of Newcastle upon Tyne, United Kingdom (UK). Special thanks to Prof. Stephanie Glendinning and Prof. David Manning for their guidance during the research at the University of Newcastle upon Tyne, UK. The XRCT scans by Durham University School of Engineering and Computing Sciences, UK is gratefully acknowledged. Thanks to Stuart Patterson and Fred Beadle for their support in the Lab, Bernard Bowler for TG-DSC-QMS analysis, and Philip Green for CEC analysis (Newcastle University, UK). The supply of lime by Buxton Lime Industries Ltd is appreciated.

REFERENCES

Al-Mukhtar, M., Khattab, S. and Alcover, J. F. (2012) Microstructure and geotechnical properties of lime-treated expansive clayey soil. Engineering Geology, 139, pp.17-27.

Beckett, C.T.S., Hall, M.R. and Augarde, C.E. (2013) Macrostructural changes in compacted earthen construction materials under loading. *Acta Geotechnica, 8*(4), pp.423-438.

BSI (2018) BS 1924-2: Hydraulically bound and stabilized materials for civil engineering purposes Part 2: Sample preparation and testing of materials during and after treatment. British Standards Institution, Milton Keynes.

BSI (2016).BS 1377. 'Methods of test for Soils for Civil Engineering Purposes', British Standards Institution, Milton Keynes, Uk,

BSI (1995a) BS 7755-3.4: Soil quality. Chemical methods. Determination of specific electrical conductivity. BSI, Milton Keynes.

Rasband, W.S. (2002) NIH Image J. http://imagej.nih.gov/ij/index html, verified 2 August, 2011.

BSI (1995b) BS 7755-3.10: Soil quality. Chemical methods. Determination of carbonate content, volumetric method. BSI, Milton Keynes.

Article DOI: 10.52589/IJMCE-A1HGJX8L
DOI URL: https://doi.org/10.52589/IJMCE-A1HGJX8L

Cizer, Ö, Van Balen, K. and Van Gemert, D. (2010). Competition between Hydration and Carbonation in Hydraulic Lime and Lime-pozzolana Mortars. *Advanced Materials Research* Vols. 133-134, pp. 241-246.

De Silva, P., Bucea, L., Moorehead, D. R. and Sirivivatnanon, V. (2006). Carbonate Binders: Reaction Kinetics, Strength and Microstructure. *Cement and Concrete Composites*, 28(7), pp.613-620.

Dorr, A. (2016) Technological change and climate scenarios. Nature Climate Change, 6, pp.638-639.

Eades, J. L., Nichols Jr, F. P. and Grim, R.E. (1962). Formation of New Minerals with Lime Stabilization as Proven by Field Experiments in Virginia. *Highway Research Board Bulletin*, 335, pp. 31-39.

Iorliam, A. Y. (2019). *Carbon capture potential in modified soil* (Doctoral dissertation, Newcastle University).

Iorliam, A.Y. UFe, M. M. and Anum, B. (2021). Carbon Capture Potential in Lime Modified Kaolin Clay. *International Journal of Engineering and Technology*, Vol. 13, No. 6, pp. 147-163.

ImageJ (2016) ImageJ Principles. [online] Available at: https://imagej.net/Principles [Accessed 12 December, 2016].

Jung, C. and Bobet, A. (2008) Post-construction evaluation of lime-treated soils.

Ketcham, R.A. and Carlson, W.D. (2001) Acquisition, optimization and interpretation of X-ray computed tomographic imagery: applications to the geosciences. *Computers & Geosciences*, *27*(4), pp.381-400

Khryashchev, V.V., Priorov, A.L., Apalkov, I.V. and Zvonarev, P.S. (2005) Image denoising using adaptive switching median filter. In IEEE International Conference on Image Processing 2005 (Vol. 1, pp. I-117). IEEE.

Lal, R. (2004) Soil carbon sequestration to mitigate climate change. Geoderma, 123(1), pp.122.

Matsushita, F., Aono Y., and Shibata, S. (2000). Carbonation Degree of Autoclaved Aerated Concrete. *Cement and Concrete Research*, 30(11), pp.1741-1745.

Nakarai, K. and Yoshida, T. (2015). Effect of Carbonation on Strength Development of Cement Treated Toyoura Silica Sand. *Soils and Foundations*, 55(4), pp.857-865.

Smith, J. (2015) Examining soil based construction materials through X-Ray computed tomography (Doctoral dissertation, Durham University).

Smith, J. and C. Augarde (2014). XRCT scanning of unsaturated soils: Microstructure at different scales? Proceedings of the TC105 ISSMGE International symposium on Geomechanics from Micro to Macro, 1137–1142.

Rogers, C.D.F., Glendinning, S. and Roff, T.E.J. (1997) Lime modification of clay soils for construction expediency. *Proceedings of the Institution of Civil Engineers-Geotechnical Engineering*, *125*(4), pp.242-249.

Washbourne, C. L., Lopez-Capel, E., Renforth, P., Ascough, P. L. and Manning, D. A. C. (2015) Rapid removal of atmospheric CO_2 by urban soils. *Environmental Science & Technology*, 49(9), pp.5434-5440.

Yi, Y., Lu, K., Liu, S. and Al-Tabbaa, A. (2015) Property changes of reactive magnesia–stabilized soil subjected to forced carbonation. Canadian Geotechnical Journal, 53(2), pp.314325.

Article DOI: 10.52589/IJMCE-A1HGJX8L
DOI URL: https://doi.org/10.52589/IJMCE-A1HGJX8L